Traveling plateaus for a hyperbolic Keller-Segel system with attraction and repulsion: existence and branching instabilities

Benoît Perthame [*] Christian Schmeiser [†] Min Tang [*‡] Nicolas Vauchelet [*§]

September 26, 2010

Abstract

How can repulsive and attractive forces, acting on a conservative system, create stable traveling patterns or branching instabilities? We have proposed to study this question in the framework of the hyperbolic Keller-Segel system with logistic sensitivity. This is a model system motivated by experiments on cell communities auto-organization, a field which is also called socio-biology. We continue earlier modeling work, where we have shown numerically that branching patterns arise for this system and we have analyzed this instability by formal asymptotics for small diffusivity of the chemo-repellent.

Here we are interested in the more general situation, where the diffusivities of both the chemo-attractant and the chemo-repellent are positive. To do so, we develop an appropriate functional analysis framework. We apply our method to two cases. Firstly we analyze steady states. Secondly we analyze traveling waves when neglecting the degradation coefficient of the chemo-repellent; the unique wave speed appears through a singularity cancelation which is the main theoretical difficulty. This shows that in different situations the cell density takes the shape of a plateau.

The existence of steady states and traveling plateaus are a symptom of how rich the system is and why branching instabilities can occur. Numerical tests show that large plateaus may split into smaller ones, which remain stable.

Key-words. Keller-Segel system, hyperbolic system, traveling waves, branching instability, cell communities.

AMS Subjects Class. 35L45, 35L67, 65M99, 92C17

1 Introduction

We study a form of the hyperbolic Keller-Segel system with logistic sensitivity for a chemoattractant and constant sensitivity for a chemo-repellent, given by the set of equations

$$\begin{cases} \partial_t n + \operatorname{div}\left[\mu_c n\left(1-\frac{n}{n_{max}}\right)\nabla c - \mu_S n \nabla S\right] = 0\,, \\ -D_c\Delta c + \frac{c}{\tau_c} = \alpha_c n\,, \\ \partial_t S - D_S \Delta S + \frac{S}{\tau_S} = \alpha_S n\,. \end{cases} \tag{1}$$

[*]UPMC, CNRS UMR 7598, Laboratoire Jacques-Louis Lions, F-75005, Paris and INRIA Paris-Rocquencourt, Equipe BANG. Email: benoit.perthame@upmc.fr

[†]Institute for Mathematics, University of Vienna, Nordbergstraße 15, 1090 Vienna, Austria and RICAM, Linz, Austria. Email: christian.schmeiser@univie.ac.at

[‡]Email: tangmin1002@gmail.com

[§]Email: nicolas.vauchelet@upmc.fr

This system is reminiscent of a large class of models used with biomedical motivations to represent the auto-organization of cells that are able to produce attractive and repulsive chemicals [8, 18], but also in other areas of population dynamics [4, 15]. The logistic sensitivity $\mu_c(1 - n/n_{max})$ takes into account a volume filling (or quorum sensing) effect, i.e., a reduction of the cell response to the chemo-attractant (whose concentration is denoted by c), which prevents overcrowding [10, 19, 20]. The special form at hand has been proposed in [5] as a reduced model for a more detailed system to study complex patterns as the dendritic ramification of *Bacillus subtilis*, recently obtained with high nutrient experiments in [11, 12, 14], whereas pattern formation based on local nutrient depletion is also possible [16, 8, 17]. It includes a chemo-repellent of concentration S (that can be interpreted as the effect of surfactin) with a constant sensitivity μ_S. The model neglects diffusion (i.e. random motion) of the cells. This has been proved to be mathematically correct, due to the logistic sensitivity, in [7, 6] (see also [2] for an earlier work). Reaction-diffusion models are used for the chemicals with a quasi-stationarity assumption for the chemo-attractant. The chemicals diffuse with diffusivities D_c and D_S, they are degraded with relaxation times τ_c and τ_S, and they are produced by the cells with rates α_c and α_S.

From [3, 2, 7] we know that, when $S \equiv 0$, the nonlinear term $n(1 - n/n_{max})$ causes sharp fronts that connect alternatively the states $n = 0$ and $n = n_{max}$ (see [9] for this terminology). The repellent force ∇S can generate surprising dynamics of the plateaus and branching instabilities may occur. This was shown in [5], and the instability could be analyzed for D_S small, because the limiting system with $D_S = 0$ can be recast as an hyperbolic system according to a method introduced in [13]. Then, stability/instability of discontinuities can be seen as a transition from shock to rarefaction waves.

In the present paper, we are interested in the existence and branching instabilities of traveling plateau solutions of (1) for general diffusion coefficients. These are naturally obtained in one dimension and therefore we focus on the nondimensionalized system

$$\begin{cases} \partial_t n + \partial_x\big(n(1-n)\partial_x c - n\partial_x S\big) = 0\,, \\ -D_c\partial_x^2 c + c = \alpha_c n\,, \\ \partial_t S - D_s\partial_x^2 S + S = \alpha_S n\,. \end{cases} \tag{2}$$

For the nondimensionalization, τ_S has been chosen as the reference time and n_{max} as the reference cell density. The reference values for the chemical densities have been chosen such that the scaled versions of the sensitivities μ_c and μ_S are equal to 1. All quantities in (2) are dimensionless. This is also true for the parameters D_c, D_S, α_c, and α_S, where we point out that the scaled diffusivities D_c and D_S actually represent (in unscaled notation) $D_c\tau_c/l^2$ and $D_S\tau_S/l^2$, respectively, where l is the reference length.

We develop a functional analytic framework for the study of traveling waves. Since it is simpler to introduce it for steady states of (2), we address this issue in Section 2. We prove the existence of a family of steady states characterized by the size of the plateau, when it is small enough, or when D_S is close enough to D_c (Section 3). Numerical tests illustrate that the smallness condition is necessary for stability. In Section 4, we show that steady states are replaced by traveling plateaus, when degradation of the chemo-repellent is neglected (i.e. $\tau_S = \infty$ in (1)). The method is an extension of the functional analytic framework for steady states, where the propagation speed is determined naturally by a singularity analysis. The total number of cells (or the size of the plateau) defines a family of traveling waves with different speeds.

2 Steady states with small total mass

The existence of stationary states for system (2) is both the most natural question and the easiest to illustrate the method we use throughout the paper. Therefore we begin with this issue. We first state a theoretical result that involves a smallness condition. Then, we confirm with numerical results that this smallness condition is necessary.

We shall look for solutions of the steady state system

$$\begin{cases} \partial_x\big(n(1-n)\partial_x c - n\partial_x S\big) = 0\,, \\ -D_c\partial_x^2 c + c = \alpha_c n\,, \\ -D_s\partial_x^2 S + S = \alpha_S n\,, \end{cases} \tag{3}$$

complemented with the boundary conditions

$$n(\pm\infty) = c(\pm\infty) = s(\pm\infty) = 0\,. \tag{4}$$

Integration of the first equation then gives vanishing flux:

$$n\big[(1-n)\partial_x c - \partial_x S\big] = 0\,.$$

We shall be interested in plateaus of the cell density with sharp boundaries, such that n jumps between $n = 0$ and

$$n = 1 - \frac{\partial_x S}{\partial_x c} > 0 \tag{5}$$

(satisfying the Rankine-Hugoniot jump conditions). The convexity of the flux function is determined by the sign of $\partial_x c$. The above jumps satisfy the entropy condition if either $n = 0$ on the left, $n > 0$ on the right of the jump, and $\partial_x c > 0$ at the jump point; or $n > 0$ on the left, $n = 0$ on the right, and $\partial_x c < 0$.

Theorem 2.1 *Assume that $\gamma := \frac{\alpha_S D_c}{\alpha_c D_S} < 1$. Then, for L small enough, there exists a unique entropy solution of* (3) *of the form*

$$n(x) = \begin{cases} 0 & \text{for } \ x \notin [0, L], \\ 1 - \gamma + O(L) & \text{for } \ x \in (0, L), \end{cases}$$

with $n \in C(0, L)$ and symmetric around $x = L/2$.

For the existence of steady state plateau solutions, we need the effect of the chemo-attractant to dominate the effect of the chemo-repellent. In terms of the original unscaled parameters, $\gamma = \frac{\alpha_S \mu_S}{D_S}\,\frac{D_c}{\alpha_c \mu_c}$ holds. Thus, the strength of the attractive (respectively repulsive) effect is measured by the product of the production rate and the sensitivity divided by the diffusivity of the chemical.

One can understand the occurrence of the free parameter L as the result of mass conservation in the dynamics (2). Supposedly there is a one-to-one relation between L and the total number of cells. This is also the way plateaus of different size are produced in the numerical examples below.

Proof of Theorem 2.1

The difficulty in using (5) for the computation of the cell density is to control the points where $\partial_x c$ vanishes. By the symmetry assumption, one such point is at $x = L/2$, and we shall prove that for n of the form given in the theorem, it is the only one.

It will be convenient to rescale the problem by $x \to Lx$. Then, the support of n is given by $[0, 1]$, where (5) still holds, and

$$\begin{cases} -\frac{D_c}{L^2}\partial_x^2 c + c = \alpha_c n\,, \\ -\frac{D_S}{L^2}\partial_x^2 S + S = \alpha_S n\,. \end{cases} \tag{6}$$

With the boundary conditions (4), explicit representations of $\partial_x c$ and $\partial_x S$ can be computed for $x \in \mathbb{R}$:

$$\partial_x c = -\frac{\alpha_c L_c^2}{2}\left(\int_0^x e^{L_c(y-x)} n(y)dy - \int_x^1 e^{L_c(x-y)} n(y)dy\right), \tag{7}$$

$$\partial_x S = -\frac{\alpha_S L_S^2}{2}\left(\int_0^x e^{L_S(y-x)} n(y)dy - \int_x^1 e^{L_S(x-y)} n(y)dy\right), \tag{8}$$

with $L_S = L/\sqrt{D_S}$, $L_c = L/\sqrt{D_c}$. Thus the formula (5) can be seen as the fixed point equation

$$n = \mathcal{F}[n] := 1 - \gamma\frac{F[L_S, n]}{F[L_c, n]}\,, \tag{9}$$

with

$$F[L_i, n](x) = -\int_0^x e^{L_i(y-x)} n(y)dy + \int_x^1 e^{L_i(x-y)} n(y)dy\,, \qquad 0 < x < 1\,, \quad i = S, c\,. \tag{10}$$

Using the symmetry at $x = 1/2$, i.e., $n(x) = n(1-x)$ for $x \in (0, 1)$, we restrict to $x \in (0, 1/2)$ and write

$$F[L_i, n](x) = e^{L_i x}\int_x^{1/2}\left(e^{-L_i y} + e^{-L_i(1-y)}\right) n(y)dy + \left(e^{-L_i(1-x)} - e^{-L_i x}\right)\int_0^x e^{L_i y} n(y)dy\,. \tag{11}$$

As the next step, the limit as $L_i \to 0$ is taken out, and the zero at $x = 1/2$ is eliminated by

$$\frac{F[L_i, n](x)}{1/2 - x} = 2\bar{n}(x) + L_i f[L_i, n](x)\,,$$

with

$$\bar{n}(x) = \frac{1}{1/2 - x}\int_x^{1/2} n(y)dy\,,$$

$$f[L_i, n](x) = \frac{1}{1/2 - x}\int_x^{1/2} \frac{e^{L_i(x-y)} + e^{L_i(x+y-1)} - 2}{L_i} n(y)dy + \frac{e^{-L_i(1-x)} - e^{-L_i x}}{L_i(1/2 - x)}\int_0^x e^{L_i y} n(y)dy\,.$$

Since $L = 0$ implies $L_i = 0$, the unique solution of (9) in this case is given by

$$n(x) = n_0 := 1 - \gamma\,.$$

We shall apply the Banach fixed point theorem in the ball

$$B := \left\{ n \in C([0, 1/2]) : \ \|n - n_0\|_\infty < \frac{1-\gamma}{2} \right\}, \tag{12}$$

of the Banach space $C([0, 1/2])$ (equipped with the supremum norm $\|\cdot\|_\infty$). The essential observation is collected in the following result.

Lemma 2.2 *For $0 < L_i \le \bar{L}$, the linear mapping $n \mapsto f[L_i, n]$ on $C([0, 1/2])$ is bounded with a bound only depending on $\bar{L}$.*

Proof. It is easily seen that both

$$\frac{e^{L_i(x-y)} + e^{L_i(x+y-1)} - 2}{L_i} \qquad \text{and} \qquad \frac{e^{-L_i(1-x)} - e^{-L_i x}}{L_i(1/2 - x)}$$

are uniformly bounded for $0 \le x, y \le 1/2$, $0 < L_i \le \bar{L}$ with a bound $C(\bar{L})$, implying

$$\|f[L_i, n]\|_\infty \le C(\bar{L}) \left(1 + \frac{e^{\bar{L}/2}}{2}\right) \|n\|_\infty .$$

□

Corollary 2.3 *For $n \in B$ and for L small enough (recalling $L_c = L/\sqrt{D_c}$, $L_S = L/\sqrt{D_S}$),*

$$2\bar{n} + L_c f[L_c, n] \ge \frac{1 - \gamma}{2}$$

and

$$n \mapsto \mathcal{F}[n] = 1 - \gamma + \gamma \frac{L_c f[L_c, n] - L_S f[L_S, n]}{2\bar{n} + L_c f[L_c, n]}$$

maps B into itself and is a contraction with respect to $\|\cdot\|_\infty$ with a Lipschitz constant proportional to L.

This concludes the proof of Theorem 2.1.

Formal asymptotic expansion – shape of the plateau

In this section the first few terms in an asymptotic expansion of the solution of (9) will be computed. This will shed light on the shape of the non-constant correction of the cell density plateau. Some of the necessary computations are rather lengthy and will only be outlined. We start with the Taylor expansion $F[L_i, n] = F_0[n] + L_i F_1[n] + L_i^2 F_2[n] + O(L_i^3)$ with

$$F_j[n](x) = -\int_0^x \frac{(y-x)^j}{j!} n(y) dy + \int_x^1 \frac{(x-y)^j}{j!} n(y) dy .$$

This in turn leads to

$$\mathcal{F}[n] = \mathcal{F}_0[n] + L\mathcal{F}_1[n] + L^2 \mathcal{F}_2[n] + O(L^3) ,$$

with

$$\begin{aligned} \mathcal{F}_0[n] &= 1 - \gamma , \qquad \mathcal{F}_1[n] = \gamma \left(\frac{1}{\sqrt{D_c}} - \frac{1}{\sqrt{D_S}}\right) \frac{F_1[n]}{F_0[n]} , \\ \mathcal{F}_2[n] &= \gamma \left(\frac{1}{D_c} - \frac{1}{D_S}\right) \frac{F_2[n]}{F_0[n]} + \frac{\gamma}{\sqrt{D_c}} \left(\frac{1}{\sqrt{D_S}} - \frac{1}{\sqrt{D_c}}\right) \frac{F_1[n]^2}{F_0[n]^2} . \end{aligned}$$

Substitution of the ansatz $n = n_0 + Ln_1 + L^2 n_2 + O(L^3)$ into (9), re-expansion, and equating coefficients of powers of L then leads to

$$\begin{aligned} n_0 &= 1-\gamma\,, \\ n_1 &= \mathcal{F}_1[n_0] = \frac{\gamma}{2}\left(\frac{1}{\sqrt{D_S}} - \frac{1}{\sqrt{D_c}}\right)\,, \\ n_2 &= D\mathcal{F}_1[n_0]n_1 + \mathcal{F}_2[n_0] = \bar{n}_2 + \frac{\gamma}{6}\left(\frac{1}{D_c} - \frac{1}{D_S}\right)(x-1/2)^2\,, \end{aligned}$$

where $D\mathcal{F}_1$ denotes the Frechet derivative of $\mathcal{F}_1$ and $\bar{n}_2$ is a (explicitly computable) constant. The $O(L)$-correction term n_1 is constant. It is negative for $D_c < D_S$ and positive for $D_c > D_S$. The first non-constant correction occurs at $O(L^2)$. It is convex for $D_c < D_S$ and concave for $D_c > D_S$. This agrees qualitatively with the numerical results of Section 3.

Finally, we mention that it is a standard procedure to extend our rigorous results in order to justify the asymptotic expansion for n in the sense that the error $O(L^3)$ can be estimated in $C([0,1/2])$ by CL^3.

Numerical experiments

We carried out numerical tests that illustrate the analytical results and indicate that large plateaus may be unstable, depending on the relation between D_c and D_S.

We obtained numerical steady states as the limit for large times of a modified dynamics (where also the chemo-repellent is determined from a quasistationary problem), which we have chosen for its simplicity:

$$\begin{cases} \partial_t n + \partial_x\big(n(1-n)\partial_x c - n\partial_x S\big) = 0\,, \\ -D_c\partial_x^2 c + c = \alpha_c n\,, \\ -D_S\partial_x^2 S + S = \alpha_S n\,. \end{cases} \tag{13}$$

We discretize the hyperbolic equation for n by the Enquist-Osher finite volume method, which is conservative and can capture the shocks on both sides of the plateaus (see [1] for a recent introduction to the subject). The elliptic equations for c and S are solved by a finite difference method. We indeed obtained that after some transient the numerical solutions converge to a steady state.

We present three families of results in Figures 1, 2 and 3. In these pictures, the solid and dashed lines on the sub-figures at the top represent n and c respectively, while the bottom sub-figures depict S.

First we illustrate Theorem 2.1 (that is L small) in Figure 1. Here the computational domain is $[0,6]$ and the initial density is an almost centered indicator function:

$$n^0 = \mathbb{1}_{[3,3.5]}\,.$$

We observe the different shapes of the steady states supporting the formal asymptotics above. When $D_c > D_S$, the positive part of n is concave, when $D_c = D_S$ it is flat, and when $D_c < D_S$ it is convex. The leading order approximation for small L suggests the relation $M \approx L(1-\gamma)$ between the total mass M and the width of the plateau. Since M and L are not very small in these computations, this approximative relation should, however, be corrected by higher order terms. In particular, note that in the simulations leading to the right picture, $\gamma = 1$ holds, such that the leading order term does not provide any contribution to the total mass.

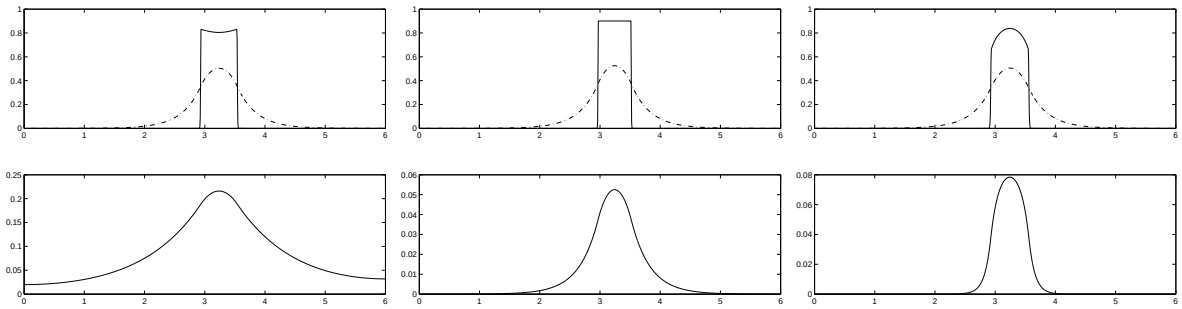

Figure 1: The steady state solution of (3) with total mass $M = 0.5$ and different chemical production rates and diffusivities. Left: $\alpha_c = 1, \alpha_S = 1, D_c = 0.1, D_S = 1$; middle: $\alpha_c = 1, \alpha_S = 0.1, D_c = 0.1, D_S = 0.1$; right: $\alpha_c = 1, \alpha_S = 0.1, D_c = 0.1, D_S = 0.01$.

Secondly, we test for L big. The numerical results for $\alpha_c = 1, \alpha_S = 1, D_c = 0.1, D_S = 1$ are presented in Figure 2, with initial data corresponding to $M = 1$, namely

$$n^0(x) = \mathbb{1}_{[2.5,3.5]}\,.$$

It seems that the total mass is too large for a one-plateau steady state to exist. The initial plateau splits into two smaller ones which appear to be stable.

It appears numerically that, when $\gamma \leq 1$, $D_c > D_S$, we always reach a steady state solution with concave cell density in the plateau, no matter how large the total mass is. As an illustration we show numerical results with $M = 2$ and the initial density

$$n^0(x) = \mathbb{1}_{[2,4]}\,.$$

The results are shown in Figure 3.

3 Steady states for almost equal diffusion lengths

Obviously, for $D_c = D_S$, i.e. $L_c = L_S$, and for $\gamma = \alpha_S/\alpha_c < 1$ the steady state problem (9) has the constant solution $n = n_0 = 1 - \gamma$ (for arbitrary $L > 0$). Note that, in terms of the original unscaled parameters (as occurring in (1)) the equality of the scaled diffusivities means equality of the quantities $\sqrt{D_c\tau_c}$ and $\sqrt{D_S\tau_S}$, which can be interpreted as diffusion lengths, i.e. the average distance a molecule diffuses, before it gets degraded.

When considering the dynamics (13) with $D_c = D_S$, it is obvious that $c\alpha_S = S\alpha_c$ holds. Therefore (13) is equivalent to

$$\begin{cases} \partial_t n + \partial_x \left(n(1-\gamma-n)\partial_x c\right) = 0\,, \\ -D_c\partial_x^2 c + c = \alpha_c n\,. \end{cases} \tag{14}$$

For $\gamma < 1$ this is exactly the problem analyzed in [7], where strong arguments for the stability of one-plateau solutions are given.

In the remainder of this section we carry out a perturbative analysis to prove existence of a plateau steady state for small values of $L_S - L_c$, and we illustrate the qualitative behaviour of the solution by a formal asymptotic expansion in terms of the perturbation parameter.

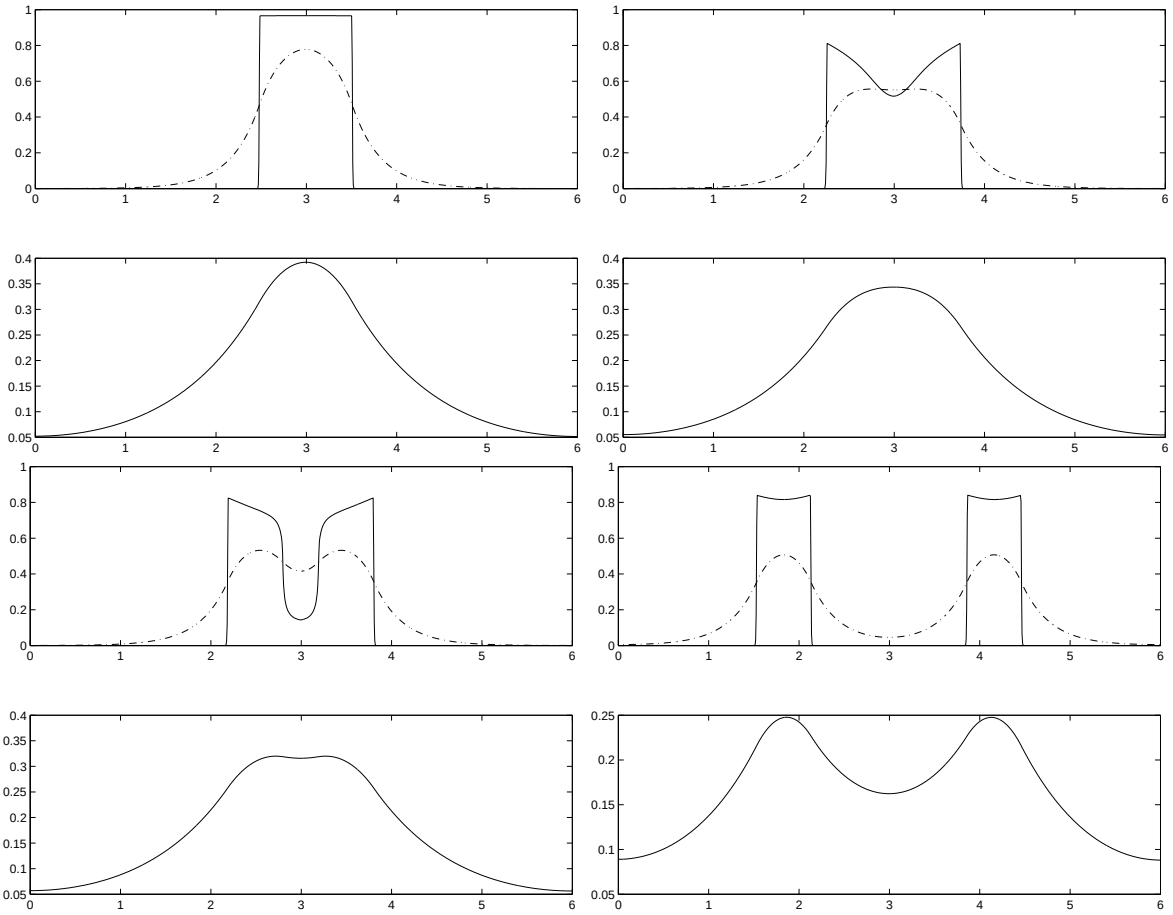

Figure 2: The instability for $D_c < D_S$ when $M = 1$. We observe that the plateau splits in two pieces, each of which stabilizes after they are well separated. In these four pairs of figures, the solid and dashed lines on the top sub-figure represent n and c, respectively, and the bottom sub-figure shows S.

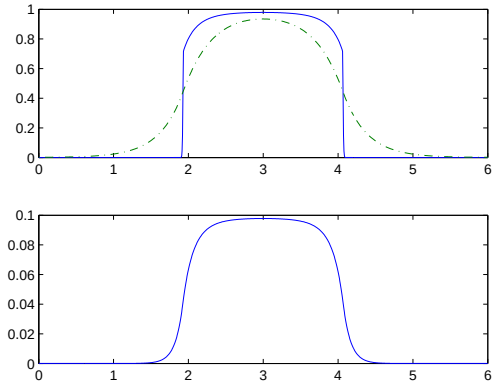

Figure 3: The stability of the plateau when $D_c > D_S$, even with $M = 2$. The parameters are $\alpha_c = 1, \alpha_S = 0.1, D_c = 0.1, D_S = 0.01$. The solid and dashed lines on the top sub-figure represent n and c respectively and the bottom sub-figure shows S.

Existence of a steady state

Our approach is completely analogous to the preceding section. We fix $L_c > 0$, introduce the perturbation parameter $\delta := L_S - L_c$, and use the decomposition (11):

$$\frac{F[L_c+\delta, n]}{1/2-x} = G[n] + \delta g[\delta, n]\,,$$

with $G[n] = F[L_c, n]/(1/2-x)$ and

$$g[\delta, n] = \frac{1}{1/2-x}\int_x^{1/2} \varphi(\delta, x, y) n(y) dy + \int_0^x \psi(\delta, x, y) n(y) dy\,,$$

where

$$\begin{aligned}
\varphi(\delta, x, y) &= \frac{e^{(L_c+\delta)(x-y)} + e^{(L_c+\delta)(x+y-1)} - e^{L_c(x-y)} - e^{L_c(x+y-1)}}{\delta}\,,\\
\psi(\delta, x, y) &= \frac{e^{(L_c+\delta)(x+y-1)} - e^{(L_c+\delta)(y-x)} - e^{L_c(x+y-1)} + e^{L_c(y-x)}}{\delta(1/2-x)}\,.
\end{aligned}$$

With this notation, the fixed point problem (9) reads

$$n = 1 - \gamma - \delta\gamma \frac{g[\delta, n]}{G[n]}\,. \tag{15}$$

So we need uniform (in δ) boundedness of the linear maps g and G, as well as boundedness away from zero of $G[n]$.

Lemma 3.1 *Let $\gamma = \alpha_s/\alpha_c < 1$ and let*

$$B := \{n \in C([0,1/2]) :\ \|n - 1 + \gamma\|_\infty < C_B\}\,, \qquad \text{with } C_B = \frac{(1-\gamma)e^{-L_c/2}}{2(2-e^{-L_c/2})}\,.$$

Then

$$G[n] \geq \frac{(1-\gamma)e^{-L_c/2}(1-e^{-L_c})}{2L_c}\,,$$

for $n \in B$ and the map G is bounded with respect to $\|\cdot\|_\infty$.

Proof. The boundedness follows immediately from the representation

$$G[n](x) = \frac{e^{L_c x}}{1/2-x}\int_x^{1/2}\left(e^{-L_c y} + e^{-L_c(1-y)}\right) n(y) dy - \frac{e^{-L_c x} - e^{-L_c(1-x)}}{1/2-x}\int_0^x e^{L_c y} n(y) dy\,.$$

Since $C_B < (1-\gamma)/2$, $n > 0$ for $n \in B$. Therefore, for $x \in (0, 1/2)$, $G[n]$ is the difference of two positive terms, and we can estimate

$$G[n](x) \geq \frac{e^{L_c x}(1-\gamma-C_B)}{1/2-x}\int_x^{1/2}\left(e^{-L_c y} + e^{-L_c(1-y)}\right) dy - \frac{e^{-L_c x} - e^{-L_c(1-x)}}{1/2-x}(1-\gamma+C_B)\int_0^x e^{L_c y} dy\,.$$

Evaluation of the integrals leads to

$$G[n](x) \geq \frac{1}{Be(L_c(2x-1))}\left[1-\gamma-C_B - (1-\gamma+C_B)\left(1-e^{-L_c x}\right)\right]\,,$$

where the Bernoulli function $Be(z) = z/(e^z-1)$ is positive and strictly decreasing. By setting $x = 0$ in its argument and $x = 1/2$ in the bracket, the lower bound from the statement of the lemma is achieved. □

Lemma 3.2 *For $0 < \delta \leq \bar{\delta}$, the linear mapping $n \mapsto g[\delta, n]$ on $C([0, 1/2])$ is bounded with a bound only depending on $\bar{\delta}$ and L_c.*

Proof. The result is a straightforward consequence of the observation that the functions φ and ψ are bounded for $\delta \in (0, \bar{\delta}]$, $x, y \in [0, 1/2)$. This again follows from the facts that their denumerators $\tilde{\varphi}(\delta, x, y)$ and, respectively, $\tilde{\psi}(\delta, x, y)$ are smooth functions of their arguments satisfying $\tilde{\varphi}(0, x, y) = \tilde{\psi}(0, x, y) = \tilde{\psi}(\delta, 1/2, y) = 0$. □

The last two results immediately imply the contraction property of the right hand side of (15) acting on B for small enough δ, which proves the following existence result.

Theorem 3.3 *Assume that $\gamma := \frac{\alpha_S}{\alpha_c} < 1$ and define $\delta = L(D_S^{-1/2} - D_c^{-1/2})$. For $|\delta|$ small enough (with L and D_c fixed), there exists a unique entropy solution of (3) of the form*

$$n(x) = \begin{cases} 0 & \text{for } x \notin [0, L], \\ 1 - \gamma + O(\delta) & \text{for } x \in (0, L), \end{cases}$$

with $n \in C(0, L)$ and symmetric around $x = L/2$.

Formal asymptotic expansion – shape of the plateau

Similarly to the preceding section we start with the expansion

$$F[L_c + \delta, n] = F[L_c, n] + \delta \hat{F}_1[L_c, n] + O(\delta^2)\,,$$

with

$$\hat{F}_1[L_c, n] = \int_0^x e^{L_c(y-x)}(x - y)n(y)dy + \int_x^1 e^{L(x-y)}(x - y)n(y)dy\,.$$

This leads to the asymptotic expansion for the cell density:

$$n = 1 - \gamma - \delta\gamma \frac{\hat{F}_1[L_c, 1 - \gamma]}{F[L_c, 1 - \gamma]} + O(\delta^2)\,.$$

A straightforward computation gives

$$n = 1 - \gamma + \delta\gamma \left(\frac{1}{L_c} + \frac{e^{-L_c x} x - e^{-L_c(1-x)}(1 - x)}{e^{-L_c x} - e^{-L_c(1-x)}} \right) + O(\delta^2)\,.$$

Differentiation and the inequality $e^{\eta} - e^{-\eta} - \eta > 0$ for $\eta > 0$ imply that the function in the parentheses is strictly increasing for $x \in (0, 1/2)$ and strictly decreasing for $x \in (1/2, 1)$. Therefore n has the same property for $\delta > 0$, i.e. $D_S < D_c$, and the opposite for $D_S > D_c$. These are the same qualitative results as in the preceding section.

4 Existence of short traveling plateaus

So far, we have proved the existence of stationary solutions, which can be viewed as traveling waves with zero velocity. In this section, we use a similar route to establish the existence of some non-zero velocity traveling plateaus. These exist when degradation of the chemo-repellent is neglected, i.e.

$\tau_S = \infty$ in (1). With an appropriate nondimensionalization and a reduction to one dimension, the system becomes

$$\begin{cases} \partial_t n + \partial_x[(1-n)n\partial_x c - n\partial_x S] = 0\,, \\ -D_c\partial_x^2 c + c = \alpha_c n\,, \\ \partial_t S - D_S\partial_x^2 S = \alpha_S n\,. \end{cases} \tag{16}$$

We consider plateaus of length L and with speed σ. They are defined as functions of the traveling wave variable $x - \sigma t$, which for simplicity is again denoted by x:

$$\begin{cases} -\sigma\partial_x n + \partial_x[(1-n)n\partial_x c - n\partial_x S] = 0\,, \\ -D_c\partial_x^2 c + c = \alpha_c n\,, \\ -\sigma\partial_x S - D_S\partial_x^2 S = \alpha_S n\,. \end{cases} \tag{17}$$

Again, we restrict our attention to solutions satisfying

$$n(x) > 0\,, \quad x \in (0, L)\,, \qquad n = 0\,, \quad \text{else.}$$

We rescale space as $x \to Lx$ and the wave speed as $\sigma \to L\sigma$ and obtain for $x \in \mathbb{R}$

$$\begin{cases} -\sigma L^2\partial_x n + \partial_x[(1-n)n\partial_x c - n\partial_x s] = 0\,, \\ -\frac{D_c}{L^2}\partial_x^2 c + c = \alpha_c n\,, \\ -\sigma\partial_x S - \frac{D_S}{L^2}\partial_x^2 S = \alpha_S n\,, \end{cases} \tag{18}$$

with

$$n > 0 \quad \text{in } (0,1)\,, \qquad n = 0 \quad \text{else.} \tag{19}$$

System (18)–(19) is defined in the whole space $x \in \mathbb{R}$ and we complete it with boundary conditions for c and S:

$$c(\pm\infty) = 0\,, \qquad S(-\infty) = S_\infty\,, \qquad S(+\infty) = 0\,. \tag{20}$$

The wave speed and the far field value S_∞ of the chemo-repellent are considered as unknown and part of the solution.

Theorem 4.1 *For $\gamma = \frac{\alpha_S D_c}{\alpha_c D_S} < 1$ and L small enough, there is a unique solution of (18)–(20), such that $n \in W^{1,\infty}(0,1)$ and*

$$n = 1 - \gamma + O(L) \quad \textit{in } (0,1)\,, \qquad \sigma = \frac{\alpha_S(1-\gamma)}{2D_S} + O(L)\,, \qquad S_\infty = 2D_S + O(L)\,.$$

Furthermore, c is concave in $(0,1)$ and S is non-increasing on $\mathbb{R}$.

The method of proof extends, with additional technicalities, that of Section 2. After integrating the equation for n, we find the following formulas for the solutions of (18)–(20):

$$n = 1 - \frac{\sigma L^2 + \partial_x S}{\partial_x c}\,, \qquad x \in [0,1], \tag{21}$$

$$\partial_x c = \frac{\alpha_c L_c^2}{2}\left(-\int_0^x e^{L_c(y-x)} n(y)dy + \int_x^1 e^{L_c(x-y)} n(y)dy\right)\,, \qquad x \in \mathbb{R}, \tag{22}$$

$$\partial_x S = -\alpha_S L_S^2 \int_0^x e^{\sigma L_S^2(y-x)} n(y)dy\,, \qquad x \in \mathbb{R}, \tag{23}$$

where, again, the notation $L_c = L/\sqrt{D_c}$, $L_S = L/\sqrt{D_S}$ has been used. If the wave speed σ was known, the right hand side of (21) could be (after substitution of (22), (23)) considered as a fixed point operator for the computation of n. The difficulty is that σ is not known a priori. The new ingredient compared to the previous sections is that σ is used to create a zero of the denumerator at the same position where it occurs in the denominator. This principle to find a traveling wave speed seems to be new.

Formally, the procedure (whose feasibility will have to be proven) is as follows: Given n, find $x_0 = x_0[n]$, such that $F[L_c, n](x_0) = 0$, with $F[L_c, n]$ as defined in (10). Then determine $\sigma = \sigma[n]$ such that

$$\sigma = \frac{\alpha_S}{D_S} \int_0^{x_0} e^{\sigma L_S^2 (y - x_0)} n(y) dy \,. \tag{24}$$

Now the cell density in the plateau can be determined as a fixed point of

$$\mathcal{F}[n](x) = 1 - \frac{2D_c}{\alpha_c} \frac{\sigma[n] - \frac{\alpha_S}{D_S} \int_0^x e^{\sigma[n] L_S^2 (y-x)} n(y) dy}{F[L_c, n](x)} \,. \tag{25}$$

The next step is to show that, for L small enough, $\mathcal{F}[n]$ is well defined on

$$B = \left\{ n \in C([0,1]) : \ \|n - 1 + \gamma\|_\infty < \frac{1-\gamma}{2} \right\} ,$$

i.e. for $(1-\gamma)/2 =: \underline{n} < n < \overline{n} := 3(1-\gamma)/2$.

Lemma 4.2 *For L_c small enough and $n \in B$ there exists a unique $x_0 = x_0[n] \in (0,1)$ satisfying $F[L_c, n](x_0) = 0$. Its dependence on n is Lipschitz:*

$$|x_0[n_1] - x_0[n_2]| \le C \|n_1 - n_2\|_\infty \,,$$

for all $n_1, n_2 \in B$, with C independent from $L_c \to 0$.

Proof. Existence follows from continuity of $F[L_c, n]$ and from $F[L_c, n](0) > 0$ and $F[L_c, n](1) < 0$. Introducing $x_j = x_0[n_j]$, $j = 1, 2$, the equation $F[L_c, n_j](x_j) = 0$ can be written as

$$\int_0^{x_j} e^{L_c y} n_j(y) dy = e^{2L_c x_j} \int_{x_j}^1 e^{-L_c y} n_j(y) dy \,, \qquad j = 1, 2 \,.$$

The difference of these two equations is written in the form

$$\begin{aligned} &\int_{x_2}^{x_1} \left(e^{L_c y} + e^{L_c (2x_2 - y)} \right) n_1(y) dy + \left(e^{2L_c x_2} - e^{2L_c x_1} \right) \int_{x_1}^1 e^{-L_c y} n_1(y) dy \\ &= \int_0^{x_2} e^{L_c y} (n_2(y) - n_1(y)) dy + e^{2L_c x_2} \int_{x_2}^1 e^{-L_c y} (n_1(y) - n_2(y)) dy \,. \end{aligned}$$

Now the modulus of the left hand side is estimated from below in terms of $|x_1 - x_2|$ and the right hand side from above:

$$\left(\underline{n} - 2L_c e^{L_c} \overline{n} \right) |x_1 - x_2| \le 2 e^{L_c} \|n_1 - n_2\|_\infty \,.$$

Since the coefficient on the left hand side can be made positive by choosing L_c small enough, this concludes the proof. □

Lemma 4.3 *Let the assumptions of Lemma 4.2 be satisfied. Then there exists a unique $\sigma = \sigma[n]$ satisfying (24) with $x_0 = x_0[n]$. Its dependence on n is Lipschitz:*

$$|\sigma[n_1] - \sigma[n_2]| \le C\|n_1 - n_2\|_\infty \,,$$

for all $n_1, n_2 \in B$, with C independent from $L_S, L_c \to 0$. Furthermore,

$$\frac{\alpha_S(1-\gamma)}{2D_S} e^{-L_S\overline{\sigma}} =: \underline{\sigma} \le \sigma \le \overline{\sigma} := \frac{3\alpha_S(1-\gamma)}{2D_S} \,.$$

Proof. Existence and uniqueness of a positive solution follow immediately from the fact that the right hand side of (24) is positive, bounded, and nonincreasing as a function of σ. The upper bound is a consequence of $n \in B$, and so is the lower bound (in the derivation of which the upper bound is also used). Similarly to the proof of Lemma 4.2, for $n_1, n_2 \in B$ the difference between the corresponding σ-equations can be written as

$$\begin{aligned}
&\sigma_1 - \sigma_2 - \frac{\alpha_S}{D_S}\int_0^{x_1}\left(e^{\sigma_1 L_S(y-x_1)} - e^{\sigma_2 L_S(y-x_1)}\right) n_1(y)dy = \frac{\alpha_S}{D_S}\int_{x_2}^{x_1} e^{\sigma_2 L_S(y-x_2)} n_1(y)dy \\
&+\frac{\alpha_S}{D_S}\int_0^{x_1}\left(e^{\sigma_2 L_S(y-x_1)} - e^{\sigma_2 L_S(y-x_2)}\right) n_1(y)dy + \frac{\alpha_S}{D_S}\int_0^{x_2} e^{\sigma_2 L_S(y-x_2)}(n_1(y) - n_2(y))dy \,.
\end{aligned}$$

It is now straightforward to estimate

$$|\sigma_1 - \sigma_2| \le C\left(|x_1 - x_2| + \|n_1 - n_2\|_\infty\right) \,,$$

and to complete the proof by using Lemma 4.2. □

With the definitions of $x_0[n]$ and $\sigma[n]$, the fixed point operator can be written as

$$\mathcal{F}[n] = \mathcal{G}[x_0[n], \sigma[n], n]$$

with notations where the singularity cancelation at x_0 appears more clearly

$$\begin{aligned}
\mathcal{G}[x_0,\sigma,n] &= 1 - 2\gamma\frac{I[x_0,n] + g[x_0,\sigma,n]}{2I[x_0,n] + f[x_0,n]} \,, \qquad I[x_0,n](x) = \int_x^{x_0} n(y)dy \,, \\
g[x_0,\sigma,n](x) &= \int_0^{x_0}\left(e^{\sigma L_S^2(y-x_0)} - 1\right) n(y)dy - \int_0^{x}\left(e^{\sigma L_S^2(y-x)} - 1\right) n(y)dy \\
&= \int_x^{x_0}\left(e^{\sigma L_S^2(y-x_0)} - 1\right) n(y)dy + \int_0^{x}\left(e^{\sigma L_S^2(y-x_0)} - e^{\sigma L_S^2(y-x)}\right) n(y)dy \,, \\
f[x_0,n](x) &= F[n](x) - F[n](x_0) - 2I[x_0,n](x) = \int_x^{x_0}\left(e^{L_c(y-x_0)} + e^{L_c(x_0-y)} - 2\right) n(y)dy \\
&\quad + \int_0^{x}\left(e^{L_c(y-x_0)} - e^{L_c(y-x)}\right) n(y)dy + \int_x^{1}\left(e^{L_c(x-y)} - e^{L_c(x_0-y)}\right) n(y)dy \,.
\end{aligned}$$

Since f and g vanish for $L = 0$ ($\Rightarrow L_S = L_c = 0$), the constant $n_0 = 1 - \gamma$ is the only fixed point in this case. The following properties of I, f and g are obtained by straightforward computations.

Lemma 4.4 *For $n \in B$ there exists a constant C independent from $L \to 0$, such that*

$$\frac{1}{2}(1-\gamma) \le \frac{I[x_0,n](x)}{x_0 - x} \le \frac{3}{2}(1-\gamma) \,, \tag{26}$$

$$\left|g[x_0,\sigma,n](x)-(x-x_0)g[x_0,\sigma,n]'(x)\right|\le CL^2(x-x_0)^2\,, \tag{27}$$

$$\left|f[x_0,n](x)-(x-x_0)f[x_0,n]'(x)\right|\le CL(x-x_0)^2\,, \tag{28}$$

$$\left|f[x_0,n]'(x)\right|\le CL\,,\qquad \left|g[x_0,\sigma,n]'(x)\right|\le CL^2\,. \tag{29}$$

Moreover C only depends on $\|n\|_\infty\le\bar n$ and not on n'.

Since we already have the Lemmas 4.2 and 4.3, we only need to examine the dependence of $\mathcal{G}[x_0,\sigma,n]$ on its arguments for proving the contraction property of $\mathcal{F}$. Unfortunately, it will turn out that the Lipschitz constant of $\mathcal{G}$ as a function of x_0 involves the derivative of n with respect to x. Therefore, we shall need a stricter definition of the set, where the fixed point iteration is carried out.

Lemma 4.5 *There exists a positive constant κ such that, for L small enough, the fixed point operator $\mathcal{F}$ maps both B into itself and the set*

$$\hat B=\left\{n\in B:\ n\in W^{1,\infty}([0,1]),\ \|n'\|_\infty\le\kappa L\right\}$$

into itself.

Proof. We use the alternative representation

$$\mathcal{F}[n]=1-\gamma-\gamma\frac{2g[x_0[n],\sigma[n],n]-f[x_0[n],n]}{2I[x_0[n],n]+f[x_0[n],n]} \tag{30}$$

and the controls

$$\frac{I[x_0,n](x)}{x_0-x}\ge\frac{1-\gamma}{2},\qquad \frac{2I(x)+f(x)}{x_0-x}\ge\frac{1-\gamma}{2}-CL. \tag{31}$$

As a first step, our previous result, together with the estimate for $\sigma[n]$ in Lemma 4.3, after cancellation of $x-x_0$ in the denominator and the denumerator, gives

$$|\mathcal{F}[n]-1+\gamma|\le\frac{CL}{1-\gamma-CL}.$$

This implies that, for small enough L, $\mathcal{F}$ maps B into itself. The second step is to compute the x-derivative of the fixed point operator:

$$\mathcal{G}[x_0,\sigma,n]'=2\gamma\frac{I'(2g-f)-I(2g'-f')+f'g-g'f}{(2I+f)^2} \tag{32}$$

For estimating this term, we need (27), (28) and the corresponding property of I. This is a first time when the derivative of n enters:

$$\left|I[x_0,n](x)-(x-x_0)I[x_0,n]'(x)\right|\le\left|\int_x^{x_0}n(y)dy-(x_0-x)n(x)\right|\le\frac{1}{2}(x-x_0)^2\|n'\|_\infty\,.$$

With these properties, for $n\in\hat B$, the modulus of the denumerator in (32) can be estimated from above by $CL(1+\kappa L)(x-x_0)^2$. On the other hand, the denominator can be estimated from below by $(1-\gamma-CL)^2(x-x_0)^2$. Thus, the bound on the derivative is preserved by $\mathcal{F}$, if

$$\frac{C(1+\kappa L)}{(1-\gamma-CL)^2}\le\kappa\,.$$

This holds for any $\kappa>C(1-\gamma)^{-2}$ and small enough L. □

Lemma 4.6 *For L small enough, $0 < x_{01}$, $x_{02} < 1$, σ_1, σ_2 satisfying the bounds in Lemma 4.3, and n_1, $n_2 \in \hat{B}$,*

$$\|\mathcal{G}[x_{01}, \sigma_1, n_1] - \mathcal{G}[x_{02}, \sigma_2, n_2]\|_\infty \leq CL \left(|x_{01} - x_{02}| + |\sigma_1 - \sigma_2| + \|n_1 - n_2\|_\infty \right) ,$$

with C independent from L. Moreover C only depends on $\|n\|_\infty \leq \bar{n}$ and not on n'.

Proof. For analyzing the dependence of $\mathcal{G}[x_0, \sigma, n]$ on x_0, it is convenient to observe the identity $\mathcal{G}[x_0, \sigma, n](x) = \mathcal{G}[x, \sigma, n](x_0)$, following from the skew symmetry of $I[x_0, n](x)$, $f[x_0, n](x)$, and $g[x_0, \sigma, n](x)$ with respect to x and x_0. It implies

$$\frac{d}{dx_0} \mathcal{G}[x_0, \sigma, n](x) = \mathcal{G}[x, \sigma, n]'(x_0) .$$

A bound of the form CL of this quantity has been shown in the proof of the previous lemma.

From the definition of $g[x_0, \sigma, n]$ it is obvious that the derivative with respect to σ is $O(L^2)$.

Finally, $I[x_0, \cdot](x)$, $f[x_0, \cdot](x)$ and $g[x_0, \sigma, \cdot](x)$ are linear functionals with the obvious bounds

$$\left\| \frac{I[x_0, n]}{x - x_0} \right\|_\infty \leq \|n\|_\infty , \quad \left\| \frac{f[x_0, n]}{x - x_0} \right\|_\infty \leq CL\|n\|_\infty , \quad \left\| \frac{g[x_0, \sigma, n]}{x - x_0} \right\|_\infty \leq CL^2\|n\|_\infty .$$

Considering again the representation (30) and the lower bound (31), the proof is completed. □

Combining the Lemmas 4.2, 4.3, 4.5, 4.6 shows that, for L small enough, $\mathcal{F} : \hat{B} \to \hat{B}$ is a contraction, completing the proof of the existence and uniqueness statement of Theorem 4.1. The limit as $L \to 0$ of n follows from the form (30) of the fixed point operator. Using this limit in the limit of the equation $F[L_c, n](x_0) = 0$ shows that the limit of x_0 is $1/2$. Then the limit of σ is obtained from $L_S \to 0$ in (24), and the limit of the far-field value S_∞ is derived by using (23):

$$S_\infty = S(-\infty) = S(0) = -\int_0^\infty \partial_x S(x) dx \to 2D_S .$$

This completes the proof of Theorem 4.1.

5 Numerical simulation of traveling plateaus

Algorithm

In the previous section, the existence of traveling wave solutions of system (16) in the form of short enough cell density plateaus has been proven. In the following, numerical simulations of system (16) will be presented, indicating the necessity of the shortness assumption for the dynamic stability of traveling plateaus.

In order to obtain fast enough convergence to a traveling wave, while it moves through the finite computational domain $[0, A]$, an approximation of the wave, corresponding to the limit $L \to 0$, is used as initial condition.

More precisely, the initial cell density $n(t = 0)$ is chosen as

$$n_0 = (1 - \gamma) \mathbb{1}_{(1, 1+L)} , \tag{33}$$

where we recall that $\gamma = \frac{\alpha_S D_c}{\alpha_c D_S}$. With this cell density, the maximum of the chemo-attractant concentration occurs at $x_0 = 1 + L/2$, and the velocity σ is obtained by solving the nonlinear equation (24). Next, an initial datum S_0 for the chemo-repellent concentration is computed by solving the equation for S in (17) (see also (23)).

Since the numerical scheme is restricted to a finite computational domain $[0, A]$, we need to define appropriate boundary conditions. Simulation times $T > 0$ are chosen such that the set $\{x,\ n(t,x) > 0\}$ stays away from the boundary points $x = 0, A$ for $0 \le t \le T$ and, since the equation for n is hyperbolic, it is enough to use zero entering flux boundary conditions.

For the chemical concentrations, Robin boundary conditions are used, which are satisfied exactly by traveling plateau solutions:

$$\sqrt{D_c}\,\partial_x c(t,0) = c(t,0)\,, \qquad \sqrt{D_c}\,\partial_x c(t,A) = -c(t,A)\,, \tag{34}$$

$$\partial_x S(t,0) = 0\,, \qquad D_S \partial_x S(t,A) + \sigma S(t,A) = 0\,. \tag{35}$$

The value of σ needs to be updated for each time step. This requires the computation of $\sigma[n]$ as described in the previous section, where the cell density n from the previous time step is used. The nonlinear equations for $x_0[n]$ and $\sigma[n]$ are solved by the Newton method.

As in Section 2, the equation for n is discretized by the Enquist-Osher scheme and the quasi-stationary equation for c by finite differences. For the parabolic equation for S a finite difference space discretization is used with time implicit treatment of the diffusion term.

Numerical results

Effect of L: In all our simulations, the computational domain is $[0, 6]$, i.e. $A = 6$. For the fixed choice of parameters

$$\alpha_c = 1, \quad \alpha_S = 1, \quad D_c = 0.1, \quad D_S = 1,$$

we take different values for the length of the initial plateau. For $L = 0.1$, 0.4, and 0.7, the evolution of n, c, and S is plotted in Figures 4, 5, and 6, respectively. We observe that, when $L = 0.1$ or 0.4, the solution converges to a plateau traveling wave. Note the differences in the plotted times between the two figures, indicating the different wave speeds. For the largest value of L, the initial plateau splits into two pieces that travel independently (with speeds dictated by their post-splitting lengths). An interesting question (we do not have an answer to) is, whether a dynamically unstable traveling wave still exists.

Plateau shapes for different physical constants: Different parameters can give different shapes for the plateau. Figure 7 depicts the detailed shape of the plateau depending on the diffusion coefficient of the chemical. It seems that when D_c (and therefore γ) increases, the plateau becomes larger and layers appear on the edges of the plateau. In this case, attraction forces decrease and therefore cells diffuse more in the middle.

Convergence of the scheme: We recall that the wave velocity $\sigma[n]$ is computed in each time step. The numerical values are displayed in Figure 8 for two different values of L. It seems that the value of σ computed from the initial data is already very close to its steady state value. Though there are small oscillations, when the mesh is refined, the amplitude of the oscillations is reduced, indicating convergence of the numerical method. It is easy to see that, regardless of the oscillations, σ is almost constant. Specifically, its value is close to $\frac{\alpha_S}{2D_S} L(1-\gamma)$ in accordance with Theorem 4.1.

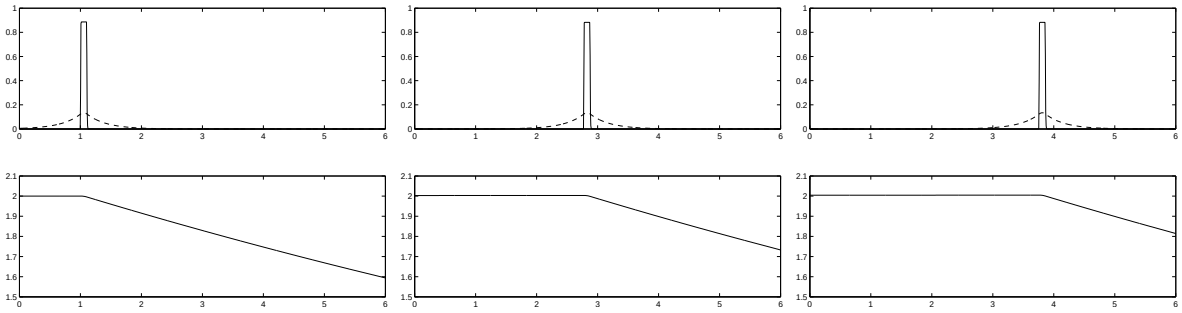

Figure 4: The solution of (16) with $L = 0.1$ for three different times. Top: The solid and dashed lines are n and c, respectively. Bottom: the evolution of S. Left: $t = 0$, middle: $t = 49.1$, right: $t = 81.9$.

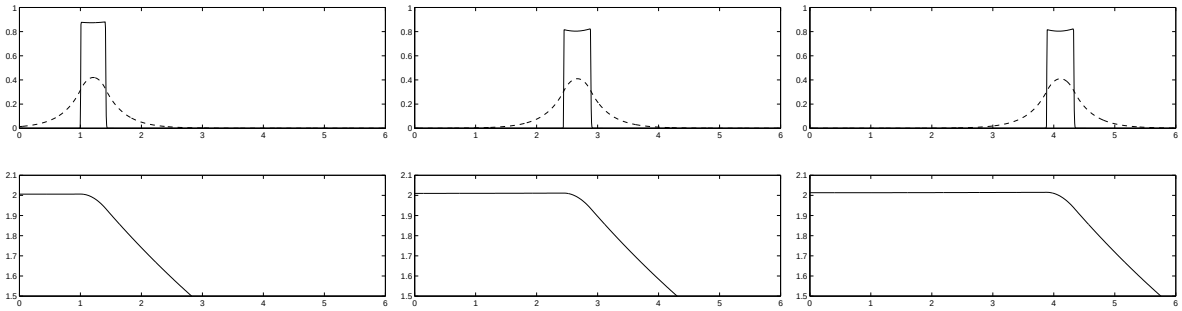

Figure 5: Same as Figure 4 with $L = 0.4$. The plotting times are now, left: $t = 0$, middle: $t = 8.1$, right: $t = 17.8$.

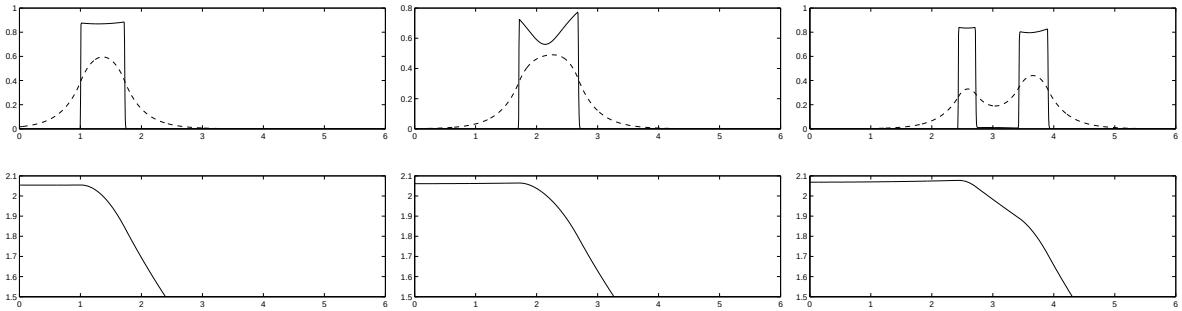

Figure 6: Same as Figure 4 with $L = 0.7$. The plotting times are now, left: $t = 0.07$, middle: $t = 3.55$, right: $t = 6.77$.

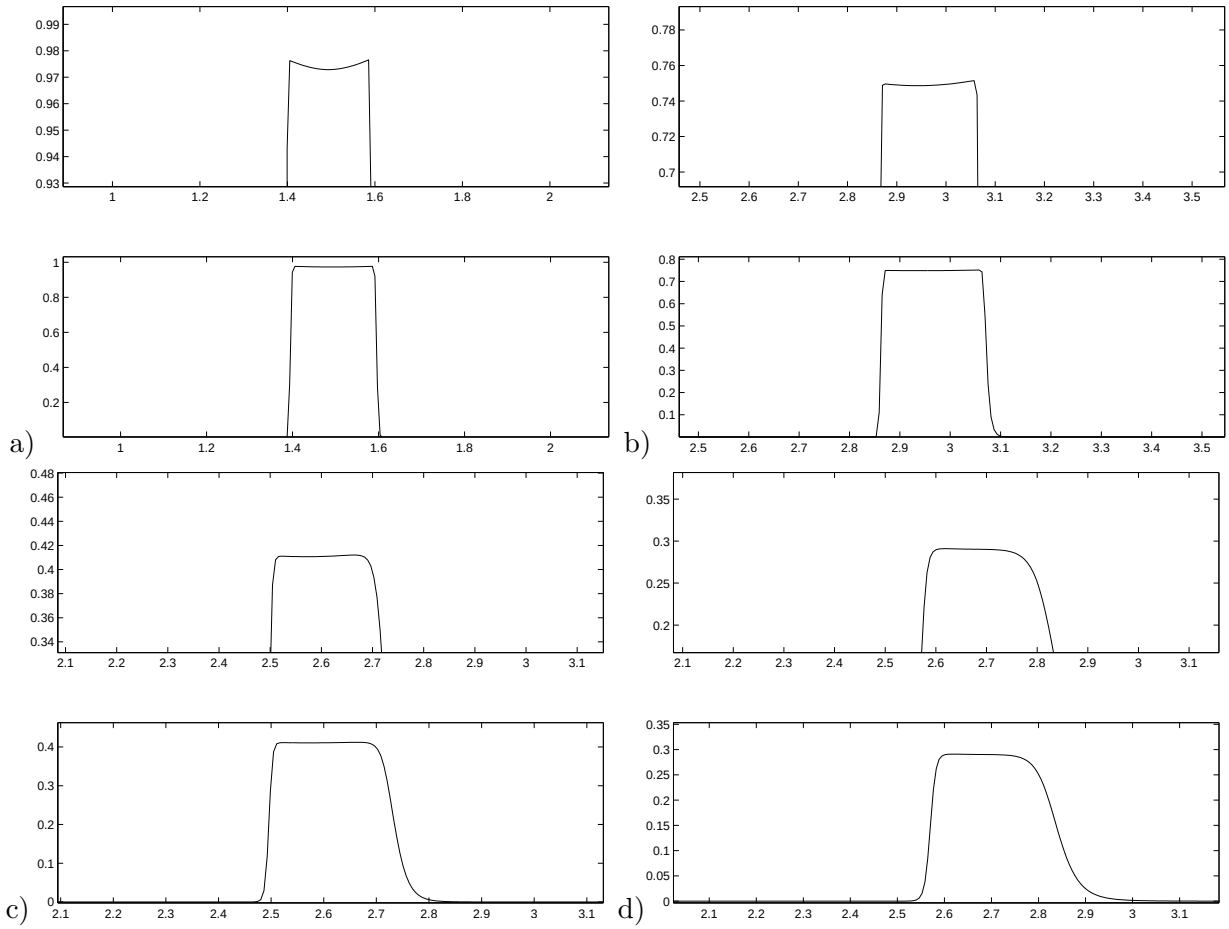

Figure 7: Different shapes of traveling plateaus. In each figure, the top subplot depicts a zoom of the peak, while the bottom subplot displays the whole plateau. Parameter values: $L = 0.2$, $\alpha_c = \alpha_S = D_S = 1$; a) $D_c = 0.01$, b) $D_c = 0.2$, c) $D_c = 0.5$, d) $D_c = 0.6$.

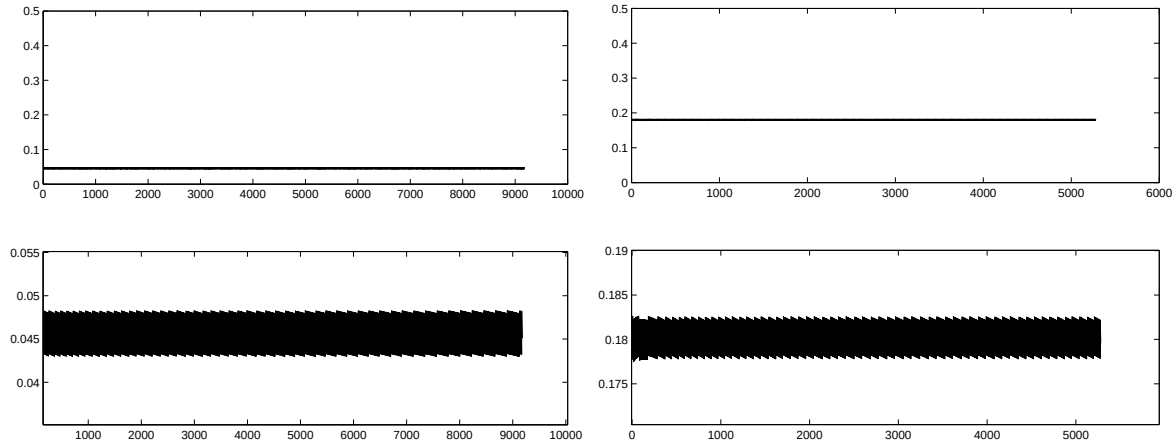

Figure 8: The velocity of the traveling plateau σ for different values of L with the parameters $\alpha_c = 1, \alpha_S = 1, D_c = 0.1, D_S = 1$. We can see that, regardless of the numerical effect, they are almost constant. Left: $L = 0.1$; right: $L = 0.4$. Top: the full scale, bottom: zoom on the oscillations.

Acknowledgment. This work was initiated, when C. S. was visiting the INRIA/UPMC team Bang on a visitor position, and completed, when C.S. and M.T. where visitors at the Newton Institute of the University of Cambridge.

References

[1] Bouchut F., *Nonlinear stability of finite volume methods for hyperbolic conservation laws and well-balanced schemes for sources*. Series Frontiers in Mathematics, Birkhäuser Verlag, Basel (2004).

[2] M. Burger, M. Di Francesco, Y. Dolak-Struss, The Keller-Segel model with prevention of overcrowding: linear vs. nonlinear diffusion. SIAM J. Math. Anal. **38** No. 4, (2006) 1288-1315.

[3] M. Burger, Y. Dolak-Struss, C. Schmeiser, Asymptotic analysis of an advection-dominated chemotaxis model in multiple spatial dimensions. Commun. Math. Sci. **6** No. 1,(2008) 1-28.

[4] M. Burger, P. Markowich, J.-F. Pietschmann. Work in preparation.

[5] F. Cerretti, B. Perthame, C. Schmeiser, M. Tang, N. Vauchelet. Waves for an hyperbolic Keller-Segel model and branching instabilities. Report INRIA-0049089 (2010). To appear in M3AS.

[6] A. L. Dalibard, B. Perthame, Existence of solutions of the hyperbolic Keller-Segel model. Trans. Amer. Math. Soc. **361** No. 5, 2319-2335 (2009).

[7] Y. Dolak-Struss, C. Schmeiser, The Keller-Segel model with logistic sensitivity function and small diffusivity. SIAM J. Appl. Math., **66** No. 1, (2005) 286-308.

[8] I. Golding, Y. Kozlovsky, I. Cohen, E. Ben-Jacob, Studies of bacterial branching growth using reaction-diffusion models for colonial development. Physica A **260**, (1998) 510-554.

[9] T. Hillen, A classification of spikes and plateaus. SIAM Rev. **49**(1), 35-51 (2007).

[10] T. Hillen, K. Painter, A user's guide to PDE models for chemotaxis. J. Math. Biol. **58**, 183-217 (2009).

[11] D. Julkowska, M. Obuchowski, I. B. Holland, S. J. Seror, Branched swarming patterns on a synthetic medium formed by wild type Bacillus subtilis strain 3610. Microbiology **150**, 1839-1849 (2004).

[12] D. Julkowska, M. Obuchowski, I. B. Holland, S. J. Seror, Comparative analysis of the development of swarming communities Bacillus subtilis 168 anda a natural wild type: critical effect of the surfactin and the composition of the medium. J. Bacteriol. **187**, 65-74 (2005).

[13] T. Li, Z. Wang, Nonlinear stability of traveling waves to a hyperbolic-parabolic system modeling chemotaxis. SIAM J. Appl. Math.**70**(5), 1522–1541 (2009).

[14] A. Marrocco, H. Henry, I. B. Holland, M. Plapp, S. J. Séror, B. Perthame, Models of self-organizing bacterial communuities and comparisons with experimental observations. Math. Model. Nat. Phenom. Mathematical Modelling of Natural Phenomena Vol. 5 No 1 (2010), 148–162.

[15] B. Maury, A. Roudneff-Chupin, F. Santambrogio, A macroscopic crowd motion model of gradient flow type. M3AN to appear.

[16] M. Mimura, H. Sakaguchi, M. Matsushita, Reaction diffusion modeling of bacterial colony patterns. Physica A, **282**, 283-303 (2000).

[17] J.D. Murray, Mathematical biology, Vol. 2, Second edition. Springer, 2002.

[18] K.J. Painter, P. Maini, and H. Othmer, Development and application of a model of cellular response to multiple chemical cues. J. Math. Biol., 41(4):285?314, 2000.

[19] K.J. Painter and T. Hillen, Volume-Filling and Quorum Sensing in Models for Chemosensitive Movement Canadian Applied Mathematics Quarterly, Vol 10(4), 2002, 501-543.

[20] B. Perthame, *Transport equations in Biology* (LN Series Frontiers in Mathematics), Birkhauser, (2007).